Identifying Cardiac Amyloid in Aortic Stenosis: ECV Quantification by CT in TAVR Patients

Research Article

Paul R Scully (MBBS MRes)[1,2], Kush P Patel (MBBS BSc)[1,2], Bunny Saberwal (MBBS)[1], Ernst Klotz (Diply Phys)[3], João B Augusto (MD)[1,2], George D Thornton (MBBS BSc)[1], Rebecca K Hughes (MBBS)[1,2], Charlotte Manisty (PhD)[1,2], Guy Lloyd (MD)[1,2,9], James D Newton (MBChB, MD)[4], Nik Sabharwal (DM)[4], Andrew Kelion (DM)[4], Simon Kennon (MD)[1], Muhiddin Ozkor (MBBS MD)[1], Michael Mullen (MBBS MD)[1], Neil Hartman (PhD)[5], João Cavalcante (MD)[6], Leon J Menezes (BA BM BCh)[1,7,8], Philip N Hawkins (PhD)[9], Thomas A Treibel (PhD)[1,2], *James C Moon (MD)[1,2], *Francesca Pugliese (PhD)[1,10,11]

*Denotes joint last author

1. Barts Heart Centre, St Bartholomew's Hospital, UK.
2. Institute of Cardiovascular Sciences, University College London, UK.
3. Siemens Healthineers, Forchheim, Germany.
4. John Radcliffe Hospital, Oxford University Hospitals, UK.
5. Nuclear Medicine, Swansea Bay UHB, UK.
6. Minneapolis Heart Institute, Minnesota, United States.
7. Institute of Nuclear Medicine, University College London, UK.
8. NIHR University College London Hospitals Biomedical Research Centre.
9. National Amyloidosis Centre, University College London, UK.
10. William Harvey Research Institute, Queen Mary University of London, UK.
11. NIHR Barts Biomedical Research Centre, UK.

Address for correspondence:
Dr Francesca Pugliese
Barts Heart Centre
St. Bartholomew's Hospital,
West Smithfield, London EC1A 7BE
Telephone: +44 20 7882 6906
Email: f.pugliese@qmul.ac.uk

Word count: 4,995 words (including figures and tables)

Disclosures: PRS is supported by a British Heart Foundation Clinical Research Training Fellowship (FS/16/31/32185). KPP is supported by an unrestricted educational grant from Edwards Lifesciences. TAT is supported by a clinical lecturer grant by the National Institute of Health Research (NIHR, UK). BS is supported by an educational grant from Siemens Healthineers. EK works for Siemens Healthineers. MM has received grants and personal fees from Edwards Lifesciences and personal fees from Abbotts Vascular. JCM is directly and indirectly supported by the UCLH NIHR Biomedical Research Centre and Biomedical Research Unit at UCLH and Barts, respectively. FP has received research support from Siemens Healthineers and this work forms part of the translational research portfolio of the NIHR Cardiovascular Biomedical Research Centre at Barts Heart Centre, which is supported and funded by the NIHR. The remaining authors have no relevant disclosures.

Key words: aortic stenosis, cardiac amyloidosis, extracellular volume, computed tomography

ABSTRACT

Background: Occult transthyretin cardiac amyloid with aortic stenosis (AS-amyloid) affects 1 in 7 elderly patients referred for transcatheter aortic valve replacement (TAVR). Bone scintigraphy with exclusion of a plasma cell dyscrasia can diagnose transthyretin-related cardiac amyloid non-invasively, for which novel treatments are emerging. Amyloid interstitial expansion increases the myocardial extracellular volume (ECV). We hypothesised CT measured ECV (ECV_{CT}) as part of routine work-up could detect AS-amyloid.

Methods: Patients with severe AS underwent bone scintigraphy (Perugini grade 0 negative; 1-3 increasingly positive) and routine TAVR-workup CT with ECV_{CT} using 3- and 5-minute post-contrast acquisitions. 20 non-AS control patients also had ECV_{CT} performed using the 5-minute post-contrast acquisition.

Results: 109 patients (43% male, 86±5 years) with severe AS and 20 controls were recruited. 16 (15%) had AS-amyloid on bone scintigraphy (5 grade 1; 11 grade 2). ECV_{CT} was 32±3%, 34±4% and 43±6% in Perugini grade 0, 1 and 2 respectively ($p<0.001$ for trend) with controls lower than lone AS (28±2%, $p<0.001$). ECV_{CT} accuracy for AS-amyloid detection versus lone AS was 0.87 (0.95 for DPD Perugini grade 2 only), outperforming conventional ECG and echocardiography parameters. One composite parameter: the voltage/mass ratio had utility (similar AUC of 0.87 for any cardiac amyloid detection), although in 1/3 of patients this could not be calculated due to bundle branch block or ventricular paced rhythm.

Conclusion: ECV_{CT} during routine CT TAVR work-up can reliably detect AS-amyloid, and the measured ECV_{CT} tracks the degree of infiltration. Another measure of interstitial expansion, the voltage/mass ratio also performed well.

ABBREVIATIONS

AS	-	Aortic stenosis
AS-amyloid	-	Dual aortic stenosis and cardiac amyloid pathology
ATTR-CA	-	Transthyretin-related cardiac amyloidosis
DPD	-	^{99m}Tc-3,3-diphosphono-1,2-propanodicarboxylic acid
ECV	-	Extracellular volume
ECV_{CT}	-	Extracellular volume quantification by computed tomography
hsTnT	-	High-sensitivity troponin T
MCF	-	Myocardial contraction fraction
NT-proBNP	-	N-terminal pro-brain natriuretic peptide
S-L criteria	-	Sokolow-Lyon criteria
TAVR	-	Transcatheter aortic valve replacement
V/M ratio	-	Voltage/mass ratio

BACKGROUND

Aortic stenosis (AS) is the most common valve disease in the developed world [1]. Its prevalence increases with age, with 2.8-4.8% of patients aged 75 and over having at least moderate AS [2,3]. Once symptomatic with severe AS, outcomes are poor without intervention [4], which can be either surgical or transcatheter aortic valve replacement (TAVR). TAVR numbers are increasing fast worldwide with both ageing populations and technological development [5,6].

Another disease of aging is wild-type transthyretin-related cardiac amyloidosis, with deposits present within the myocardium in up to 25% of patients aged 85 and over at autopsy [7]. Recent work has shown a remarkably high prevalence (14-16%) of transthyretin-related cardiac amyloidosis (ATTR-CA) in the elderly AS population being considered for TAVR – AS-amyloid [8,9]. We do not yet fully understand the significance of this dual pathology, either for valve intervention or the role for specific amyloid therapies such as tafamidis [10], patisiran [11] and inotersen [12], but detection is likely to be important. Conventional first-line investigations for ATTR-CA, such as echocardiography, blood biomarkers or the ECG are confounded by the dual pathology. ATTR-CA can now be diagnosed non-invasively using bone scintigraphy – such as ^{99m}Tc-3,3-diphosphono-1,2-propanodicarboxylic acid (DPD), ^{99m}Tc-pyrophosphate (PYP) and ^{99m}Tc-hydroxymethylene diphosphonate (HMDP) – coupled with a negative search for a plasma cell dyscrasia [13]. Although availability and awareness are increasing, it requires an extra test in elderly, often frail patients.

As part of routine TAVR work-up, patients typically undergo contrast computed tomography (CT) to assess annulus dimensions, coronary artery height (and patency, where possible) and vascular access. Contrast CT can also be used to measure the myocardial extracellular volume (ECV) in a manner similar to cardiovascular magnetic resonance (CMR) [14,15]. The ECV increases moderately with diffuse fibrosis, but massively with amyloidosis [16]. Our group has previously validated ECV quantification by CT (ECV_{CT}) against CMR and histology (endomyocardial biopsy) in severe AS [17,18] and against CMR in cardiac amyloid [18]. Unlike recommended CMR acquisition, the ECV_{CT} acquisition for cardiac amyloid can be performed earlier at five rather than ten minutes post-contrast [18].

We hypothesised that ECV_{CT} as part of routine TAVR work-up CT, would be able to detect AS-amyloid. To improve workflow, we also sought to optimise the scanning protocol in terms of dose and timing (shortened scan delay).

METHODS

This work represents prespecified analysis of a subset of patients of ATTRact-AS (*a study investigating the role of occult cardiac amyloid in the elderly with aortic stenosis,* NCT03029026). Relevant local ethics were obtained. Patients aged 75 and over with severe AS referred for TAVR at Barts Heart Centre (BHC) and undergoing CT as part of their clinical work-up were included in this sub-study. The only exclusion criterion was being unable to provide informed consent. Patients underwent routine clinical TAVR workup including baseline electrocardiogram (ECG), echocardiography and CT. The additional research procedures were DPD scintigraphy (prior to TAVR), the additional CT acquisitions for ECV_{CT}, and, if not already performed, contemporaneous blood tests for hematocrit, high-sensitivity troponin T (hs-TnT) and N-terminal pro-brain natriuretic peptide (NT-proBNP). There were 20 control patients who also underwent ECV_{CT}. These were recruited for a separate study evaluating ECV_{CT} in patients with suspected coronary artery disease and all had contemporary CMR demonstrating normal biventricular size and function with no late gadolinium enhancement. These control patients were included to provide an estimate of 'normal' ECV_{CT} and were *not* used in the screening calculations.

Electrocardiogram

Sokolow-Lyon criteria were calculated as the sum of the amplitude of the S-wave in lead V1 and the R-wave in lead V5 or V6 (whichever was greater) [19]. The voltage/mass ratio was defined as the Sokolow-Lyon total divided by the indexed left ventricular (LV) mass on echocardiography. Patients with bundle branch block or a ventricular paced rhythm were excluded from this analysis [20]. Low limb lead voltages were defined as all limb leads with an amplitude $\leq$ 0.5mV.

Echocardiography

Clinical transthoracic echocardiogram (TTE) assessed AS severity (aortic valve peak velocity, mean gradient, and valve area), other valve pathology, biventricular systolic and left ventricular diastolic function [23–25]. Left ventricular ejection fraction (LVEF) was

calculated using Simpson's biplane if possible, otherwise visually; and the indexed stroke volume (SV) using the left ventricular outflow tract (LVOT) velocity time integral and diameter, which was then indexed to BSA. Relative wall thickness was defined as: (2 x posterior wall diameter)/(LV internal diameter at end-diastole) [24]. LV mass was calculated using the formula from Devereux et al [25]:

$$\text{LV mass} = 0.8 \times 1.04 \times [(\text{IVSd} + \text{LVIDd} + \text{PWd})^3 - \text{LVIDd}^3] + 0.6$$

Where IVSd is the interventricular septal diameter, LVIDd is the left ventricular internal dimension at end-diastole and PWd is the posterior wall diameter, all measured in 2D. Longitudinal strain analysis was performed offline by an accredited echocardiographer using Tomtec Imaging Systems 2D Cardiac Performance Analysis software, Germany.

As both AS and amyloid may have myocardial impairment better captured by Myocardial Contraction Fraction (MCF = stroke volume/myocardial volume) [26], we calculated this with left ventricular end-diastolic volume (LVEDV) as 4.5 x LVIDd^2; left ventricular end-systolic volume (LVESV) as 3.72 x LVIDs^2; stroke volume as LVEDV – LVESV; LV mass as 1.04 x $[(\text{IVSd} + \text{LVIDd} + \text{PWd})^3 - \text{LVIDd}^3]$ and the myocardial volume as the LV mass / mean density of myocardium (1.04g/ml).

DPD Scintigraphy

All DPD scans were performed using either a hybrid single photon emission computed tomography (SPECT)-CT gamma camera (Phillips Brightview) or SPECT gamma camera (Siemens Symbia) following the injection of 700 MBq DPD. The imaging protocol consisted of an early and late (5 minutes and 3 hours respectively) planar whole-body image, with a SPECT/CT or SPECT only of the chest at 3 hours. DPD scans were reported by two experienced clinicians using the Perugini grading system [27], with grade 0 being negative and grades 1-3 increasingly positive. DPD scan findings were independently reviewed by the National Amyloidosis Centre (NAC). All patients with a positive DPD scan were discussed with the managing clinicians and, where appropriate, referred to the NAC for further review.

Computed Tomography

All CT scans were performed on a Somatom FORCE scanner (Siemens Healthineers, Erlangen, Germany). The TAVR work-up CT protocol at BHC involves: a topogram, calcium score, timing bolus, gated CT coronary angiogram (CTCA) acquired retrospectively and a FLASH whole body (lung apices down to the lesser trochanters). Total volume of

Omnipaque (iohexol) 300 contrast was fixed at 90mls (including the 10mls timing bolus) for the clinical scan, with no additional contrast used for research purposes. The additional acquisitions for research were a baseline 'axial shuttle mode' pre-contrast after the calcium score and further pseudo-equilibrium axial shuttle mode datasets, both triggered 250ms after the R wave, at 3- and 5-minutes post-contrast (following the FLASH whole body scan). All axial shuttle mode datasets (4 repetitions every other heartbeat, single breath hold) were acquired at a fixed tube voltage of 80kV and tube current-time product of 370mAs. Image reconstruction was performed using the same field of view in all three datasets. An additional dataset was reconstructed from the retrospectively acquired CTCA at 250ms of the R-R interval, with a field of view matching that of the axial shuttle mode datasets (figure 1) to be used as a landmark for ECV_{CT} measurement and overlay.

Extracellular Volume Analysis

Non-rigid registration software (Hepacare, Siemens Healthineers, Erlangen, Germany) allowed averaging and aligning of the axial shuttle mode datasets to improve image quality and reduce noise. The averaged baseline image was then subtracted from the averaged 3- and 5-minute post-contrast images (providing a partition coefficient) and then registered with the CTCA image. A region of interest was placed in the LV blood pool on the CTCA image and the hematocrit (usually taken on the same day) inputted, generating a myocardial ECV_{CT} map via the formula: ECV_{CT} = (1–hematocrit) x (ΔHU_{myo} /ΔHU_{blood}), where ΔHU is the change in Hounsfield unit attenuation pre- and post-contrast (i.e. $HU_{post\text{-}contrast} - HU_{pre\text{-}contrast}$) [18,28,29]. This was loaded into prototype software (Cardiac Function, Siemens Healthineers, Erlangen, Germany), which allowed the ECV_{CT} map to be superimposed on the CTCA image, the myocardial contours to be edited and the results to be displayed as a 17-segment polar map (figures 1 and 2). When calculating total ECV_{CT}, focally elevated ECV_{CT} (eg likely myocardial infarction) were not excluded, but AHA segments with significant beam hardening artefact from adjacent pacing wires (n=4) were excluded. Left ventricular (LV) mass was calculated using the standard automated software on clinical syngo.via (Siemens Healthineers, Erlangen, Germany) workstations.

Statistical analysis

Statistical analysis was performed using IBM SPSS Statistics (Version 25) software. Where appropriate, results are described as mean ± standard deviation or median (interquartile range). Kruskall-Wallis ANOVA was used when comparing more than two groups as the

omnibus test, with the Dunn-Bonferroni test for pairwise comparison. Bland Altman analysis was performed to compare 3- and 5-minute post-contrast timepoints, as well as the impact of dose reduction. Receiver operating characteristic (ROC) curve analysis was used to assess diagnostic performance. The Student's t-test or Mann-Whitney U test was used to compare continuous variables and either Chi-Squared or Fisher's Exact testing for categorical data as appropriate. Univariate and multivariate analysis was performed using binary logistic regression with the presence of AS-amyloid as the dependent variable. Variables for the multivariate analysis were selected based on statistical significance on univariate analysis and clinical relevance, while avoiding multicollinearity (e.g. only one parameter reflecting LV mass was included). Variance inflation factors for each independent variable used in the multivariate analysis were calculated as one divided by the tolerance (defined as one minus R-squared of the regression model for the studied variable). V/M ratio was not included in the multivariate analysis to avoid excluding nearly a third of patients (32 in total) with bundle branch block or ventricular paced rhythm. The DeLong test was used to compare areas under the curves (AUCs). A two-sided *p*-value <0.05 was considered statistically significant.

RESULTS

109 patients (43% male, aged 86±5 years) with severe AS were included in this sub-study of ATTRact-AS. Overall LVEF was 54±10%, peak aortic valve velocity was 4.1±0.6m/s, mean pressure gradient 41±14mmHg and aortic valve area 0.71±0.23cm^2. Patient characteristics (demographics, comorbidities, ECG, echocardiographic, CT, blood tests) are described in table 1. As might be expected, hypertension, hypercholesterolaemia, diabetes mellitus and atrial fibrillation were common in this group of patients. Venous hematocrit was 0.38±0.04, which was usually taken on the same day as the CT scan (median 0 days, IQR 0-22 days). 20 controls were also recruited separately to provide an idea of 'normal' ECV_{CT} (65% male, aged 60±11 years).

Detection of AS-amyloid

In this substudy, 16 patients (15%) had AS-amyloid diagnosed by bone scintigraphy (5 grade 1; 11 grade 2), average age 88±5 years and 56% male. A plasma cell dyscrasia was detected in 6 patients (38%), who were either referred to the NAC or reviewed with the clinical team and AL amyloid was felt unlikely in all cases. All patients genotyped so far (*n*=9, 56%) were wild-type.

There was no difference in the age (88±5 years vs 85±5 years, *p*=0.08) or proportion of male patients (56% vs 41%, *p*=0.25) when comparing AS-amyloid and lone AS. The cardiovascular risk profile (hypertension, hypercholesterolaemia and diabetes mellitus), presence of AF or permanent pacemaker pre-procedure were similar. Patients with AS-amyloid had a longer QRS duration and higher prevalence of right bundle branch block, as well as a lower EKG voltage by Sokolow-Lyon criteria and lower voltage/mass ratio. In AS-amyloid, parameters reflecting left ventricular thickness and mass were higher, whereas the MCF was lower. Global longitudinal strain was impaired in both AS-amyloid and lone AS but not different. Both hs-TnT and NT-proBNP were higher in AS-amyloid (table 1).

ECV_{CT}: ECV_{CT} was feasible for measurement in all the patients where data was obtained. ECV_{CT} was 32±3%, 34±4% and 43±6% in those patients with Perugini grade 0, 1 and 2 respectively using a 3-minute post-contrast acquisition (p<0.001 for trend) (figure 3 and central illustration). By comparison, ECV_{CT} in controls was 28±2% using a 5-minute post-contrast protocol, lower than in those patients with lone AS at similar post-contrast timing (33 ± 4%, p<0.001). For the detection of any cardiac amyloid in patients with AS (DPD Perugini grade 1 or 2), the area under the curve (AUC) was 0.87 (95% confidence interval: 0.75-0.98) using a 3-minute post-contrast acquisition (figure 4). Different ECV_{CT} thresholds could be set: 29.2% (sensitivity 100% specificity 19%, negative predictive value 100%); 31.4% (sensitivity 94%, specificity 48%, negative predictive value 98%) or 33.4% (sensitivity 88%, specificity of 66%, negative predictive value 97%). If repeated for the detection of only grade 2 AS-amyloid (as there is more uncertainty about the clinical significance of a Perugini grade 1 DPD) the AUC improved to 0.95 (95% confidence interval 0.89-1.00) and an ECV_{CT} of 33.4% offered 100% sensitivity and 64% specificity, with a negative predictive value of 100%.

Combined parameters: The voltage/mass ratio was lower in AS-amyloid and performed similar to ECV_{CT} for the detection of *any* cardiac amyloid (AUC 0.87), but not quite as well for the detection of DPD grade 2 cardiac amyloidosis (AUC 0.85). However, nearly a third of patients (32 in total) had to be excluded from this analysis due the presence of bundle branch block or a ventricular paced rhythm. MCF also performed reasonably well as a screening tool for any cardiac amyloid (AUC 0.67) - similar to PWd (AUC 0.75, *p*=0.12), but not as well as ECV_{CT} (AUC 0.87, *p*=0.003) (figure 4).

Predictors of amyloid presence: Univariate analysis identified ECV_{CT}, the presence of RBBB and parameters associated with LV wall thickness or mass (IVSd, PWd, indexed LV mass, MCF and voltage/mass ratio) as predictors of AS-amyloid (table 2). Multivariate analysis of age, ECV_{CT}, male gender, PWd and RBBB showed that only ECV_{CT} and the presence of RBBB was associated with AS-amyloid (p = 0.001 and 0.01 respectively) (table 2). For every 1% increase in ECV_{CT} there was a 1.6-fold increase in the likelihood of AS-amyloid (95% confidence interval 1.21 – 2.10). Variance inflation factors for each multivariable were all close to 1, suggesting little multicollinearity (supplementary table 3).

Protocol Optimisation:

104 patients completed both a 3- and 5-minute post-contrast acquisition. The 3-minute acquisition resulted in an acceptable ECV_{CT} result with very little bias – 0.68±1.2% lower than the 5-minute acquisition (supplementary figure 6A). This bias appears to increase above an ECV_{CT} of 40%, where such increases would not alter diagnostic accuracy.

Dose Reduction Strategy

The dose-length product (DLP) for the full baseline, 3- and 5-minute 'axial shuttle mode' datasets was 182±26mGy.cm, 183±24mGy.cm and 180±24mGy.cm respectively. To investigate dose reduction strategies, we re-analysed ECV_{CT} derived using fewer 'shuttles' (1 or 2 vs 4) for the baseline and 3-minute post-contrast acquisitions to assess any possible impact on diagnostic accuracy. Including 13 patients with lone AS and 14 patients with cardiac amyloid (9 grade 2), there was minimal bias for 1 vs 4 shuttles (0.85±2.1%) or 1 vs 2 shuttles (0.58±1.47%) (supplementary figure 6B). Two outliers with differences beyond the 95% limits of agreement were both patients weighing over 90kg, where dose modulation would likely be used clinically. Reducing the protocol to a single shuttle pre- and 3-minutes post-contrast reduces the dose by a factor of 4 (total DLP of ~90mGy.cm, effective dose 2.3mSv, using the higher cardiac k-factor of 0.026) [30].

DISCUSSION

ECV_{CT} can reliably detect dual AS-amyloid pathology in potential TAVR patients, with only an additional 3-minutes on top of the standard CT-workup and a small radiation burden (~2.3mSv), with measured ECV_{CT} not just detecting, but tracking the degree of infiltration.

The ability to detect ATTR-CA non-invasively using bone scintigraphy has led to the increased realisation that particularly wild-type ATTR-CA is not rare in the elderly. Recent work has shown just how common it is in the elderly with AS [8,9,31,32], but this is not just limited to this population – indeed 13% of patients with heart failure with preserved ejection fraction may have underlying cardiac amyloid [33] and 5% of those with LVH may have variant ATTR-CA (this study used genotyping to screen LVH patients and so will have missed those with wild-type ATTR-CA) [34]. The clinical impact of myocardial amyloid deposition in these patients with aortic stenosis however remains unclear. We know that there may be a long pre-clinical phase and that prevalence increases with age – becoming the primary cause of death in supercentenarians [35]. The spectrum therefore potentially extends from 'bystander' to the primary cause of symptoms and adverse outcome, depending on the time of diagnosis and the myocardial tolerance. In turn, these are likely to be affected by amyloid burden, rate of amyloid deposition, the ability of the myocardium to adapt, and other myocardial "hits", such as, in this case, the increased afterload from aortic stenosis. These may not be independent - the prevalence of AS-amyloid appears to be above that one would expect from age alone, suggesting that there may be an interaction – with an increased likelihood of amyloid in the interstitium of myocardium with afterload. This uncertainty of significance cascades into our terminology which is not fixed. Should this be AS-amyloid or Amyloid-AS? Similarly, cardiac amyloidosis (implies pathological) vs cardiac amyloid (may be bystander deposition). Here we have chosen AS-amyloid. These questions are about to become non-academic and pressingly so - with the availability of three novel, potential, but costly medical therapies for cardiac amyloidosis [10–12], which are yet to be validated in patients with AS-amyloid. Clearly an individualised treatment strategy is going to be needed and answers will hopefully prove more forthcoming with the increasing availability of bone scintigraphy enabling increased diagnostic rates and research activity.

The fact that pre-existing RBBB is associated with cardiac amyloidosis is intriguing and may prove relevant in the TAVR cohort given that we know that RBBB is associated with a higher likelihood of post-TAVR pacemaker implantation [36] and worse outcomes [36,37]. Although the authors did not investigate for the presence of concomitant cardiac amyloidosis, it is possible that the presence of RBBB at baseline might be an omen sign that deserves further investigation.

We propose CT as a technique to increase AS-amyloid detection and present a diagnostic algorithm (figure 5). Because ECV_{CT} is easy to implement and the patient is already in the CT scanner, we think adoption could be high. This algorithm still uses bone scintigraphy (and exclusion of AL amyloid by serum free light chains, serum and urine immunofixation) [13], but substantially increases the test yield by gate-keeping access. ECV_{CT} also seems to track cardiac amyloid burden and, as a result, may also have a future role in in monitoring response to therapy – in the same way that CMR-derived ECV can track primary light-chain (AL) cardiac amyloid regression with therapy [38]. Normal ECV_{CT} is in the region of 27% (adjusted down by 0.68±1.2% for the averaged, 3-minute post-contrast equivalent), which is consistent with the wider literature in both CT [39] and CMR [15]. Patients with lone AS had a higher ECV_{CT} (32% with an averaged, 3-minute post-contrast) likely reflecting a degree of myocardial fibrosis [15,40].

We propose different thresholds for onward referral depending on how important grade 1 vs 2 is discovered to be, and whether specificity or sensitivity becomes the priority. A lower threshold of 29% using a 3-minute post-contrast acquisition would never miss a case (sensitivity 100%), but would result in probably an unacceptably high referral rate for bone scintigraphy (specificity 19%). A threshold of 31.4% would have a sensitivity of 94% and not miss a DPD grade 2, but would miss a proportion of DPD grade 1 cases (1/5 in our cohort), however the trade-off is fewer cases would be referred for an unnecessary DPD (specificity 48%).

Technological developments often result in new insights into established techniques. We were not surprised to find that AS-amyloid was hard to detect based on ECG (such as small voltages) or echocardiographic changes (such as reduced MCF) because both AS and amyloid can have widely different impacts on heart muscle. RBBB being associated with AS-amyloid is interesting and may prove important given that we know it is both common in TAVR patients and is associated with worse outcome (including higher likelihood of post-TAVR pacemaker insertion) [36]. Another interesting finding is that a combination parameter of both ECG and echo – the voltage/mass ratio performed exceptionally well for amyloid detection compared to parameters derived from just one technique. This is perhaps not surprising as ECV_{CT} and voltage/mass ratio are effectively measuring the same thing: ECV_{CT} measures the proportional size of the water gap between myocytes and the voltage/mass ratio measures effectively the deficit of electrical depolarisation from what is expected for a

measured wall thickness – both measures of myocyte dilution by cardiac amyloid. Unfortunately, Sokolow-Lyon criteria is not validated in patients with bundle branch block [20], either native or from a ventricular paced rhythm which effectively excluded 1/3 of our patients. Furthermore, the need to combine information from two different measurement techniques is a potential barrier.

LIMITATIONS

This was a single centre, single vendor study. ECV_{CT} performance on other vendors has not been assessed, but should follow similar methodology. Focal ECV_{CT} elevations were included in the calculated global ECV_{CT} – excluding these areas may increase performance. Our mean patient age was 86. Younger cohorts will have possibly lower rates of discovered AS-amyloid. This study is a CT technical development subset of a larger study (including for example only those patients who had not already had CT at the time of recruitment) - although prevalence and other clinical information informs, this is not the primary focus of this paper. Inline ECV_{CT} software is not yet available and the work presented here will need to be optimised for integration into the daily CT workflow. Although global longitudinal strain data was included in this study, unfortunately we did not have regional longitudinal strain data available at the time of submission, which may have proven additive in identifying cardiac amyloidosis. The relatively small number of patients with AS-amyloid in this study may also have affected our results.

CONCLUSIONS

Lone AS results in detectable increases in ECV_{CT} compared to controls. ECV_{CT} using a low-dose protocol, with a 3-minute post-contrast acquisition can detect AS-amyloid and grade its severity in the TAVR population and could be used as a screening tool in those already undergoing a clinically-indicated CT.

TABLES AND FIGURES

Figure 1: ECV_{CT} protocol and offline analysis outline. Text in red represents additional image acquisition/reconstruction in scanning protocol for ECV_{CT} quantification. Text in blue represents steps in offline analysis. ASM = axial shuttle mode, ECV = extracellular volume, ECV_{CT} = extracellular volume quantification by computed tomography, recon = reconstruction and ROI = region of interest.

Figure 2: Automated heart model output with the ECV_{CT} map superimposed upon the CTCA images (**A – D**) and corresponding 3-hour planar DPD image (**E**). The endo- and epicardial contours can be edited in the short axis **(A)** four-chamber (**B**) and two-chamber views **(D)** to produce an ECV_{CT} AHA 17-segment polar map (**C**). Here, a patient with AS-amyloid (Perugini grade 2 DPD) with total myocardial ECV_{CT} is globally elevated at 47%. AHA = American Heart Association, AS = aortic stenosis, CTCA = computed tomography coronary angiography, DPD = ^{99m}Tc-3,3-diphosphono-1,2-propanodicarboxylic acid scintigraphy, ECV = extracellular volume, ECV_{CT} = extracellular volume quantification by computed tomography.

Figure 3: Box and whisker plot showing the change in ECV_{CT} at 3-minutes by DPD Perugini grade. P<0.001 for trend and for the pairwise comparison of grade 0 vs grade 2. DPD = ^{99m}Tc-3,3-diphosphono-1,2-propanodicarboxylic acid scintigraphy and ECV = extracellular volume.

Figure 4: Receiver operating characteristic (ROC) curve for the detection of *any* cardiac amyloid (DPD Perugini grade 1 or 2) using ECV_{CT} with a 3-minute post-contrast acquisition, posterior wall diameter (PWd) and myocardial contraction fraction (MCF). V/M ratio was not included as this would have excluded nearly a third of patients (32 in total) due to bundle branch block or ventricular paced rhythm. AUC = area under the curve, CI = 95% confidence interval, DPD = ^{99m}Tc-3,3-diphosphono-1,2-propanodicarboxylic acid scintigraphy, ECV = extracellular volume quantification using computed tomography.

Figure 5: Proposed ECV_{CT} screening algorithm for incorporation into routine clinical workflow. Note: algorithm can be adjusted to an ECV_{CT} threshold of ≥29% for the detection of *all* grade 1 DPD patients.

Central Illustration: ECV_{CT} polar maps (top), DPD image (middle) and axial SPECT images (bottom) from control (far left) through lone AS, DPD Perugini grade 1 and DPD Perugini grade 2 (far right).

Supplementary figure 6: Bland Altman plots comparing 3- and 5-minute post-contrast acquisitions for ECV_{CT} (**A**) and single shuttle with four shuttles (baseline and post-contrast acquisitions) for ECV_{CT} (**B**). The 95% limits of agreement are shown in red (-1.70% and 3.06% for **A**; -3.26% and 4.97% for **B**) and the mean difference is shown as the solid black line (0.68% for **A**; 0.85% for **B**). ECV = extracellular volume, ECV_{CT} = extracellular volume quantification using computed tomography.

	Overall (n=109)	Lone AS (n=93)	AS-amyloid (n=16)	*p*-value
Demographics				
Male	47 (43%)	38 (41%)	9 (56%)	0.25
Age (years)	86±5	85±5	88±5	0.08
Clinical Parameters				
Hypertension	86 (79%)	73 (78%)	13 (81%)	1.00
Hypercholesterolemia	44 (40%)	37 (40%)	7 (44%)	0.77
Diabetes Mellitus	25 (23%)	24 (26%)	1 (6%)	0.11
Atrial Fibrillation	49 (45%)	41 (44%)	8 (50%)	0.66
Permanent Pacemaker	14 (13%)	12 (13%)	2 (13%)	1.00
ECG Parameters				
Heart rate (bpm)	73±15	73±16	70±14	0.46
Low voltage limb leads	1 (1%)	1 (1%)	0 (0%)	1.00
S-L Criteria (mV)	2.5±1.0	2.6±1.0	1.8±0.5	**0.048**
1st Degree HB*	21 (19%)	20 (22%)	1 (7%)	0.30
QRS duration (ms)	106±25	103±26	120±20	**0.01**
LBBB*	10 (10%)	8 (9%)	2 (13%)	1.00
RBBB*	12 (12%)	6 (7%)	6 (38%)	**0.002**
Echo Parameters				
Left Ventricle				
LVEF (%)	54±11	54±10	58±10	0.18
Indexed SV (ml/m^2)	38±11	38±12	35±9	0.29
IVSd (cm)	1.3±0.2	1.3±0.2	1.4±0.3	**0.002**
PWd (cm)	1.1±0.3	1.1±0.2	1.3±0.3	**<0.001**
Relative wall thickness (cm)	0.50±0.15	0.48±0.13	0.61±0.20	**0.002**
Indexed LV mass (g/m^2)	116±37	113±37	137±31	**0.01**
MCF (%)	23.7±8.4	24.5±8.4	19.4±7.2	**0.02**
Mitral annulus S' (m/s)	0.06±0.01	0.06±0.01	0.05±0.01	0.08
Global LV LS (%)	-15±6	-15±7	-16±6	0.62
Diastolic Function				
E/A ratio	0.8 (0.7-1.3)	0.8 (0.7-1.1)	1.4 (0.9-2.3)	0.07
Lateral E/E'	17±10	17±8	21±15	0.28
MV Deceleration time (ms)	235±90	234±92	238±80	0.87
LA diameter (cm)	4.1±0.7	4.0±0.7	4.4±0.6	0.08
RV Function				
TAPSE (cm)	1.91±0.46	1.92±0.48	1.89±0.36	0.82
Aortic Valve				
Peak velocity (m/s)	4.10±0.63	4.12±0.63	4.02±0.62	0.55
Mean gradient (mmHg)	69±21	42±14	38±12	0.36
AVA (cm^2)	0.71±0.23	0.71±0.23	0.72±0.21	0.92

CT Parameters				
AV Calcium Score (HU)	2115 (1497-3184)	2107 (1491-3109)	2170 (1665-3602)	0.60
Indexed LV mass (g/m^2)	74±19	72±17	91±24	0.01
Composite Parameters				
V/M ratio ($mV/g/m^2$)	0.025±0.01	0.026±0.011	0.013±0.004	**<0.001**
Blood Results				
Hematocrit	0.38±0.04	0.38±0.04	0.38±0.05	0.92
Creatinine (mmol/L)	108±38	106±37	120±38	0.16
eGFR ($ml/min/1.73m^2$)	53±16	54±17	47±12	0.12
hs-TnT (ng/L)	34 (15-38)	20 (14-34)	43 (28-75)	**0.001**
NT-proBNP (ng/L)	1517 (671-3703)	1361 (593-2816)	3668 (1259-5165)	**0.03**

Table 1: Basic demographics, clinical, echocardiography and computed tomography parameters for patients with lone AS and AS-amyloid. AS = aortic stenosis, AV = aortic valve, AVA = aortic valve area, HB = heart block, eGFR = estimated glomerular filtration rate, hs-TnT = high-sensitivity troponin T, HU = Hounsfield units, IVSd – interventricular septum diameter, LS = longitudinal strain, LV = left ventricle, LBBB = left bundle branch block, LVEF = left ventricular ejection fraction, MCF = myocardial contraction fraction, NT-proBNP = N-terminal pro-brain natriuretic peptide, PWd = posterior wall diameter, RBBB = right bundle branch block, S-L = Sokolow-Lyon criteria, TAPSE = tricuspid annular plane systolic excursion, V/M = voltage mass ratio. Values represent mean ± standard deviation or median (interquartile range) where appropriate. *Missing ECG data in four lone AS and one AS-amyloid patient – percentages and statistics quoted reflect this.

Univariate Analysis			Multivariate Analysis		
Variable	**p-value**	**Exp (B)**	***p*-value**	**Exp (B)**	**CI for Exp (B)**
Age (per year increase)	0.08	1.10	0.38	1.09	0.90 – 1.30
ECV_{CT} (per % increase)	**<0.001**	1.49	**0.001**	1.60	1.21 – 2.10
AVA (per cm^2 increase)	0.92	1.12	-		
AV Mean PG (per mmHg decrease)	0.36	0.98	-		
AV Vmax (per m/s decrease)	0.55	0.77	-		
AV Calcium Score (per HU increase)	0.56	1.00	-		
E/A Ratio (per unit increase)	0.04	1.74	-		
Gender (male)	0.26	1.86	0.81	0.81	0.14 – 4.60
GLS (per % decrease)	0.61	0.98	-		
hs-TnT (per ng/L increase)	0.06	1.01	-		
Indexed LV Mass on Echo (per g/m^2 increase)	**0.02**	1.02	-		
Indexed SV (per ml/m^2 decrease)	0.28	0.97	-		
IVSd (per cm increase)	**0.005**	44.66	-		
LA Diameter (per cm increase)	0.08	2.04	-		
Lateral E/E' (per unit increase)	0.11	1.04	-		
LBBB	0.60	1.56	-		
LVEF (per % increase)	0.18	1.04	-		
MCF (per % decrease)	**0.02**	0.91	-		
Mitral Annulus S' (per m/s decrease)	0.08	0.00	-		
MV Dec Time (per ms increase)	0.87	1.00	-		
NT-proBNP (per ng/L increase)	0.41	1.00	-		
PWd (per cm increase)	**0.003**	53.83	0.46	4.04	0.10 – 162.36
RBBB	**0.001**	9.22	**0.01**	16.84	1.87 – 148.54
RWT (per cm increase)	**0.006**	178.47	-		
S-L Criteria (per mV decrease)	0.06	0.26	-		
TAPSE (per cm decrease)	0.81	0.87	-		
V/M Ratio (per $mV/g/m^2$ decrease)	**0.02**	0.00	-		

Table 2: Univariate and multivariate binary logistic regression analysis, showing that ECV_{CT} and the presence of RBBB was associated with AS-amyloid. For every 1% increase in ECV_{CT} there was a 1.6-fold increased likelihood of AS-amyloid. V/M ratio was not included in the multivariate analysis as this would have excluded nearly a third of patients (32 in total) due to bundle branch block or ventricular paced rhythm. Only one parameter representing LV wall thickness or mass was included in the multivariate analysis to avoid multicollinearity (in this case PWd, as it had the strongest association on univariate analysis). AV = aortic valve, AVA = aortic valve area, Exp (B) = exponentiation of the B coefficient, GLS = global longitudinal strain, hs-TnT = high-sensitivity troponin T, HU = Hounsfield units, LV = left ventricle, LBBB = left bundle branch block, LVEF = left ventricular ejection fraction, MCF = myocardial contraction fraction, MV = mitral valve, NT-proBNP = N-terminal pro-brain natriuretic peptide, RBBB = right bundle branch block, RWT = relative wall thickness, S-L = Sokolow-Lyon, TAPSE = tricuspid annular plane systolic excursion, V/M = voltage mass ratio.

Dependent / Independent	Age	ECV_{CT}	Gender	PWd	RBBB
Age	-	1.142	1.106	1.059	1.118
ECV_{CT}	1.056	-	1.029	1.043	1.051
Gender	1.046	1.052	-	1.078	1.064
PWd	1.040	1.107	1.119	-	1.111
RBBB	1.045	1.063	1.052	1.058	-

Supplementary Table 3: Variance inflation factors between variables included in the multivariate analysis were overall low (close to 1), suggesting little multicollinearity. ECV_{CT} = extracellular volume quantification by computed tomography, PWd = posterior wall diameter, RBBB = right bundle branch block.

REFERENCES

[1] Iung B. A prospective survey of patients with valvular heart disease in Europe: The Euro Heart Survey on Valvular Heart Disease. Eur Heart J 2003;24:1231–43. https://doi.org/10.1016/S0195-668X(03)00201-X.

[2] Thaden JJ, Nkomo VT, Enriquez-Sarano M. The Global Burden of Aortic Stenosis. Prog Cardiovasc Dis 2014;56:565–71. https://doi.org/10.1016/j.pcad.2014.02.006.

[3] Lindroos M, Kupari M, Heikkilä J, Tilvis R. Prevalence of aortic valve abnormalities in the elderly: an echocardiographic study of a random population sample. J Am Coll Cardiol 1993;21:1220–5.

[4] Turina J, Hess O, Sepulcri F, Krayenbuehl HP. Spontaneous course of aortic valve disease. Eur Heart J 1987;8:471–83.

[5] Leon MB, Smith CR, Mack MJ, Makkar RR, Svensson LG, Kodali SK, et al. Transcatheter or Surgical Aortic-Valve Replacement in Intermediate-Risk Patients. N Engl J Med 2016;374:1609–20. https://doi.org/10.1056/NEJMoa1514616.

[6] Mack MJ, Leon MB, Thourani VH, Makkar R, Kodali SK, Russo M, et al. Transcatheter Aortic-Valve Replacement with a Balloon-Expandable Valve in Low-Risk Patients. N Engl J Med 2019;380:1695–705. https://doi.org/10.1056/NEJMoa1814052.

[7] Tanskanen M, Peuralinna T, Polvikoski T, Notkola I, Sulkava R, Hardy J, et al. Senile systemic amyloidosis affects 25% of the very aged and associates with genetic variation in *alpha2-macroglobulin* and *tau* : A population-based autopsy study. Ann Med 2008;40:232–9. https://doi.org/10.1080/07853890701842988.

[8] Scully PR, Treibel TA, Fontana M, Lloyd G, Mullen M, Pugliese F, et al. Prevalence of Cardiac Amyloidosis in Patients Referred for Transcatheter Aortic Valve Replacement. J Am Coll Cardiol 2018;71:463–4. https://doi.org/10.1016/j.jacc.2017.11.037.

[9] Castaño A, Narotsky DL, Hamid N, Khalique OK, Morgenstern R, DeLuca A, et al. Unveiling transthyretin cardiac amyloidosis and its predictors among elderly patients with severe aortic stenosis undergoing transcatheter aortic valve replacement. Eur Heart J 2017;38:2879–87. https://doi.org/10.1093/eurheartj/ehx350.

[10] Maurer MS, Schwartz JH, Gundapaneni B, Elliott PM, Merlini G, Waddington-Cruz M, et al. Tafamidis Treatment for Patients with Transthyretin Amyloid Cardiomyopathy. N Engl J Med 2018;379:1007–16. https://doi.org/10.1056/NEJMoa1805689.

[11] Solomon SD, Adams D, Kristen A, Grogan M, González-Duarte A, Maurer MS, et al. Effects of Patisiran, an RNA Interference Therapeutic, on Cardiac Parameters in Patients With Hereditary Transthyretin-Mediated Amyloidosis: Analysis of the APOLLO Study. Circulation 2019;139:431–43. https://doi.org/10.1161/CIRCULATIONAHA.118.035831.

[12] Dasgupta NR, Benson M. IMPROVED SURVIVAL OF PATIENTS WITH TRANSTHYRETIN AMYLOID CARDIOMYOPATHY WITH INOTERSEN (TTR SPECIFIC ANTISENSE OLIGONUCLEOTIDE). J Am Coll Cardiol 2019;73:811. https://doi.org/10.1016/S0735-1097(19)31418-4.

[13] Gillmore JD, Maurer MS, Falk RH, Merlini G, Damy T, Dispenzieri A, et al. Nonbiopsy Diagnosis of Cardiac Transthyretin AmyloidosisCLINICAL PERSPECTIVE. Circulation 2016;133:2404–12. https://doi.org/10.1161/CIRCULATIONAHA.116.021612.

[14] Scully PR, Bastarrika G, Moon JC, Treibel TA. Myocardial Extracellular Volume Quantification by Cardiovascular Magnetic Resonance and Computed Tomography. Curr Cardiol Rep 2018;20. https://doi.org/10.1007/s11886-018-0961-3.

[15] Sado DM, Flett AS, Banypersad SM, White SK, Maestrini V, Quarta G, et al. Cardiovascular magnetic resonance measurement of myocardial extracellular volume in health and disease. Heart 2012;98:1436–41. https://doi.org/10.1136/heartjnl-2012-302346.
[16] Banypersad SM, Sado DM, Flett AS, Gibbs SDJ, Pinney JH, Maestrini V, et al. Quantification of Myocardial Extracellular Volume Fraction in Systemic AL Amyloidosis: An Equilibrium Contrast Cardiovascular Magnetic Resonance Study. Circ Cardiovasc Imaging 2013;6:34–9. https://doi.org/10.1161/CIRCIMAGING.112.978627.
[17] Bandula S, Banypersad SM, Sado D, Flett AS, Punwani S, Taylor SA, et al. Measurement of Tissue Interstitial Volume in Healthy Patients and Those with Amyloidosis with Equilibrium Contrast-enhanced MR Imaging. Radiology 2013;268:858–64. https://doi.org/10.1148/radiol.13121889.
[18] Treibel TA, Bandula S, Fontana M, White SK, Gilbertson JA, Herrey AS, et al. Extracellular volume quantification by dynamic equilibrium cardiac computed tomography in cardiac amyloidosis. J Cardiovasc Comput Tomogr 2015;9:585–92. https://doi.org/10.1016/j.jcct.2015.07.001.
[19] Sokolow M, Lyon TP. The ventricular complex in left ventricular hypertrophy as obtained by unipolar precordial and limb leads. Am Heart J 1949;37:161–86. https://doi.org/10.1016/0002-8703(49)90562-1.
[20] Hancock EW, Deal BJ, Mirvis DM, Okin P, Kligfield P, Gettes LS. AHA/ACCF/HRS Recommendations for the Standardization and Interpretation of the Electrocardiogram: Part V: Electrocardiogram Changes Associated With Cardiac Chamber Hypertrophy: A Scientific Statement From the American Heart Association Electrocardiography and Arrhythmias Committee, Council on Clinical Cardiology; the American College of Cardiology Foundation; and the Heart Rhythm Society: *Endorsed by the International Society for Computerized Electrocardiology*. Circulation 2009;119. https://doi.org/10.1161/CIRCULATIONAHA.108.191097.
[21] Baumgartner H, Hung J, Bermejo J, Chambers JB, Edvardsen T, Goldstein S, et al. Recommendations on the Echocardiographic Assessment of Aortic Valve Stenosis: A Focused Update from the European Association of Cardiovascular Imaging and the American Society of Echocardiography. J Am Soc Echocardiogr 2017;30:372–92. https://doi.org/10.1016/j.echo.2017.02.009.
[22] Wharton G, Steeds R, Allen J, Phillips H, Jones R, Kanagala P, et al. A minimum dataset for a standard adult transthoracic echocardiogram: a guideline protocol from the British Society of Echocardiography. Echo Res Pract 2015;2:G9–24. https://doi.org/10.1530/ERP-14-0079.
[23] Nagueh SF, Smiseth OA, Appleton CP, Byrd BF, Dokainish H, Edvardsen T, et al. Recommendations for the Evaluation of Left Ventricular Diastolic Function by Echocardiography: An Update from the American Society of Echocardiography and the European Association of Cardiovascular Imaging. J Am Soc Echocardiogr 2016;29:277–314. https://doi.org/10.1016/j.echo.2016.01.011.
[24] Lang RM, Badano LP, Mor-Avi V, Afilalo J, Armstrong A, Ernande L, et al. Recommendations for Cardiac Chamber Quantification by Echocardiography in Adults: An Update from the American Society of Echocardiography and the European Association of Cardiovascular Imaging. Eur Heart J – Cardiovasc Imaging 2015;16:233–71. https://doi.org/10.1093/ehjci/jev014.
[25] Devereux RB, Alonso DR, Lutas EM, Gottlieb GJ, Campo E, Sachs I, et al. Echocardiographic assessment of left ventricular hypertrophy: comparison to necropsy findings. Am J Cardiol 1986;57:450–8. https://doi.org/10.1016/0002-9149(86)90771-x.

[26] Rubin J, Steidley DE, Carlsson M, Ong M-L, Maurer MS. Myocardial Contraction Fraction by M-Mode Echocardiography Is Superior to Ejection Fraction in Predicting Mortality in Transthyretin Amyloidosis. J Card Fail 2018;24:504–11. https://doi.org/10.1016/j.cardfail.2018.07.001.
[27] Perugini E, Guidalotti PL, Salvi F, Cooke RMT, Pettinato C, Riva L, et al. Noninvasive Etiologic Diagnosis of Cardiac Amyloidosis Using 99mTc-3,3-Diphosphono-1,2-Propanodicarboxylic Acid Scintigraphy. J Am Coll Cardiol 2005;46:1076–84. https://doi.org/10.1016/j.jacc.2005.05.073.
[28] Nacif MS, Kawel N, Lee JJ, Chen X, Yao J, Zavodni A, et al. Interstitial Myocardial Fibrosis Assessed as Extracellular Volume Fraction with Low-Radiation-Dose Cardiac CT. Radiology 2012;264:876–83. https://doi.org/10.1148/radiol.12112458.
[29] Nacif MS, Liu Y, Yao J, Liu S, Sibley CT, Summers RM, et al. 3D left ventricular extracellular volume fraction by low-radiation dose cardiac CT: Assessment of interstitial myocardial fibrosis. J Cardiovasc Comput Tomogr 2013;7:51–7. https://doi.org/10.1016/j.jcct.2012.10.010.
[30] Trattner S, Halliburton S, Thompson CM, Xu Y, Chelliah A, Jambawalikar SR, et al. Cardiac-Specific Conversion Factors to Estimate Radiation Effective Dose From Dose-Length Product in Computed Tomography. JACC Cardiovasc Imaging 2018;11:64–74. https://doi.org/10.1016/j.jcmg.2017.06.006.
[31] Cavalcante JL, Rijal S, Abdelkarim I, Althouse AD, Sharbaugh MS, Fridman Y, et al. Cardiac amyloidosis is prevalent in older patients with aortic stenosis and carries worse prognosis. J Cardiovasc Magn Reson 2017;19. https://doi.org/10.1186/s12968-017-0415-x.
[32] Treibel TA, Fontana M, Gilbertson JA, Castelletti S, White SK, Scully PR, et al. Occult Transthyretin Cardiac Amyloid in Severe Calcific Aortic StenosisCLINICAL PERSPECTIVE: Prevalence and Prognosis in Patients Undergoing Surgical Aortic Valve Replacement. Circ Cardiovasc Imaging 2016;9:e005066. https://doi.org/10.1161/CIRCIMAGING.116.005066.
[33] González-López E, Gallego-Delgado M, Guzzo-Merello G, de Haro-del Moral FJ, Cobo-Marcos M, Robles C, et al. Wild-type transthyretin amyloidosis as a cause of heart failure with preserved ejection fraction. Eur Heart J 2015;36:2585–94. https://doi.org/10.1093/eurheartj/ehv338.
[34] Damy T, Costes B, Hagège AA, Donal E, Eicher J-C, Slama M, et al. Prevalence and clinical phenotype of hereditary transthyretin amyloid cardiomyopathy in patients with increased left ventricular wall thickness. Eur Heart J 2016;37:1826–34. https://doi.org/10.1093/eurheartj/ehv583.
[35] Coles LS, Young RD. Supercentenarians and transthyretin amyloidosis: The next frontier of human life extension. Prev Med 2012;54:S9–11. https://doi.org/10.1016/j.ypmed.2012.03.003.
[36] Auffret V, Webb JG, Eltchaninoff H, Muñoz-García AJ, Himbert D, Tamburino C, et al. Clinical Impact of Baseline Right Bundle Branch Block in Patients Undergoing Transcatheter Aortic Valve Replacement. JACC Cardiovasc Interv 2017;10:1564–74. https://doi.org/10.1016/j.jcin.2017.05.030.
[37] Watanabe Y, Kozuma K, Hioki H, Kawashima H, Nara Y, Kataoka A, et al. Pre-Existing Right Bundle Branch Block Increases Risk for Death After Transcatheter Aortic Valve Replacement With a Balloon-Expandable Valve. JACC Cardiovasc Interv 2016;9:2210–6. https://doi.org/10.1016/j.jcin.2016.08.035.
[38] Martinez-Naharro A, Abdel-Gadir A, Treibel TA, Zumbo G, Knight DS, Rosmini S, et al. CMR-Verified Regression of Cardiac AL Amyloid After Chemotherapy. JACC Cardiovasc Imaging 2018;11:152–4. https://doi.org/10.1016/j.jcmg.2017.02.012.

[39] Kurita Y, Kitagawa K, Kurobe Y, Nakamori S, Nakajima H, Dohi K, et al. Estimation of myocardial extracellular volume fraction with cardiac CT in subjects without clinical coronary artery disease: A feasibility study. J Cardiovasc Comput Tomogr 2016;10:237–41. https://doi.org/10.1016/j.jcct.2016.02.001.
[40] Treibel TA, López B, González A, Menacho K, Schofield RS, Ravassa S, et al. Reappraising myocardial fibrosis in severe aortic stenosis: an invasive and non-invasive study in 133 patients. Eur Heart J 2018;39:699–709. https://doi.org/10.1093/eurheartj/ehx353.

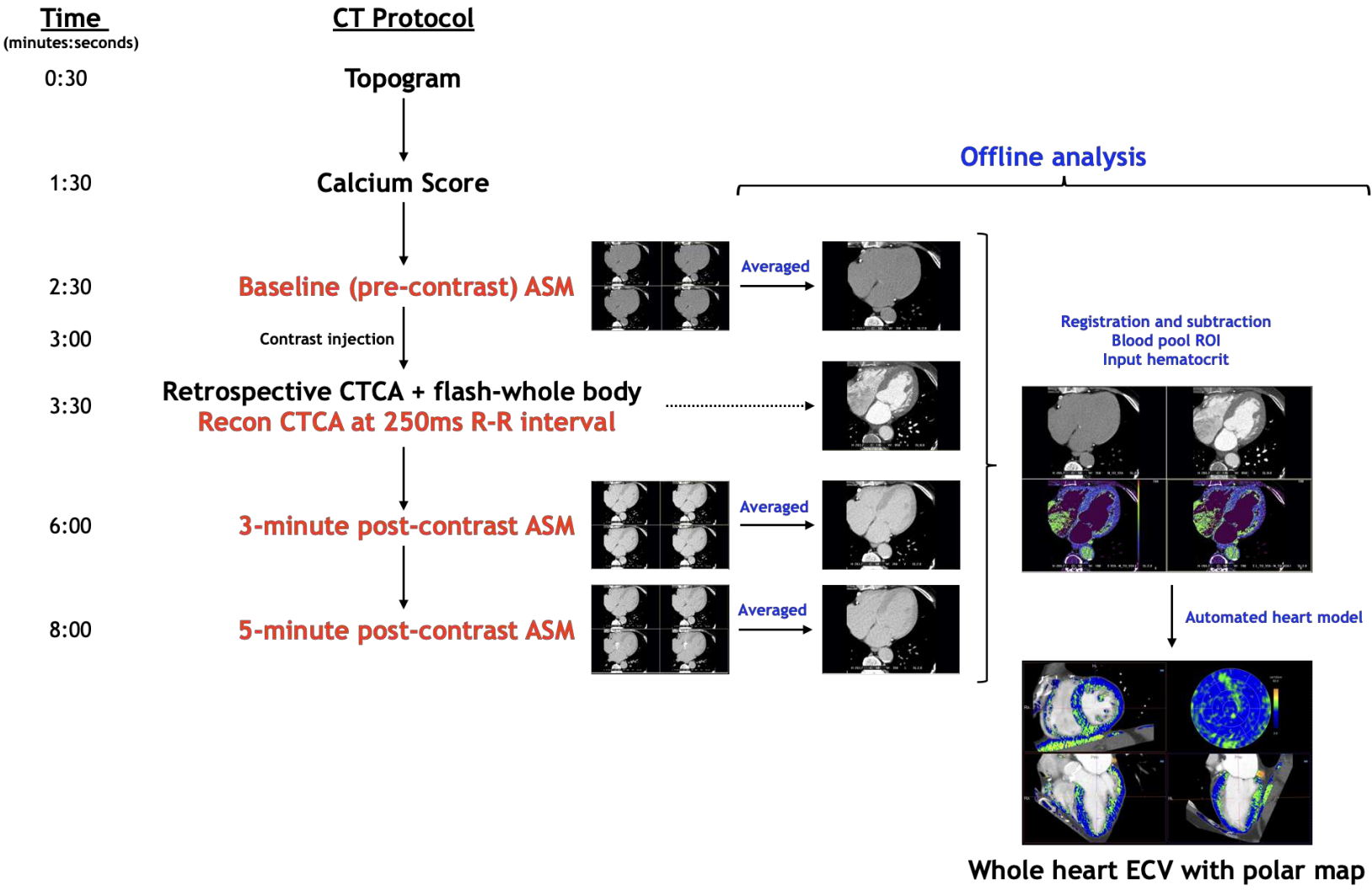
Time
(minutes:seconds)
CT Protocol
0:30
Topogram
1:30
Calcium Score
2:30
Baseline (pre-contrast) ASM
3:00
Contrast injection
3:30
Retrospective CTCA + flash-whole body
Recon CTCA at 250ms R-R interval
6:00
3-minute post-contrast ASM
8:00
5-minute post-contrast ASM
Averaged
Averaged
Averaged
Offline analysis
Registration and subtraction
Blood pool ROI
Input hematocrit
Automated heart model
Whole heart ECV with polar map

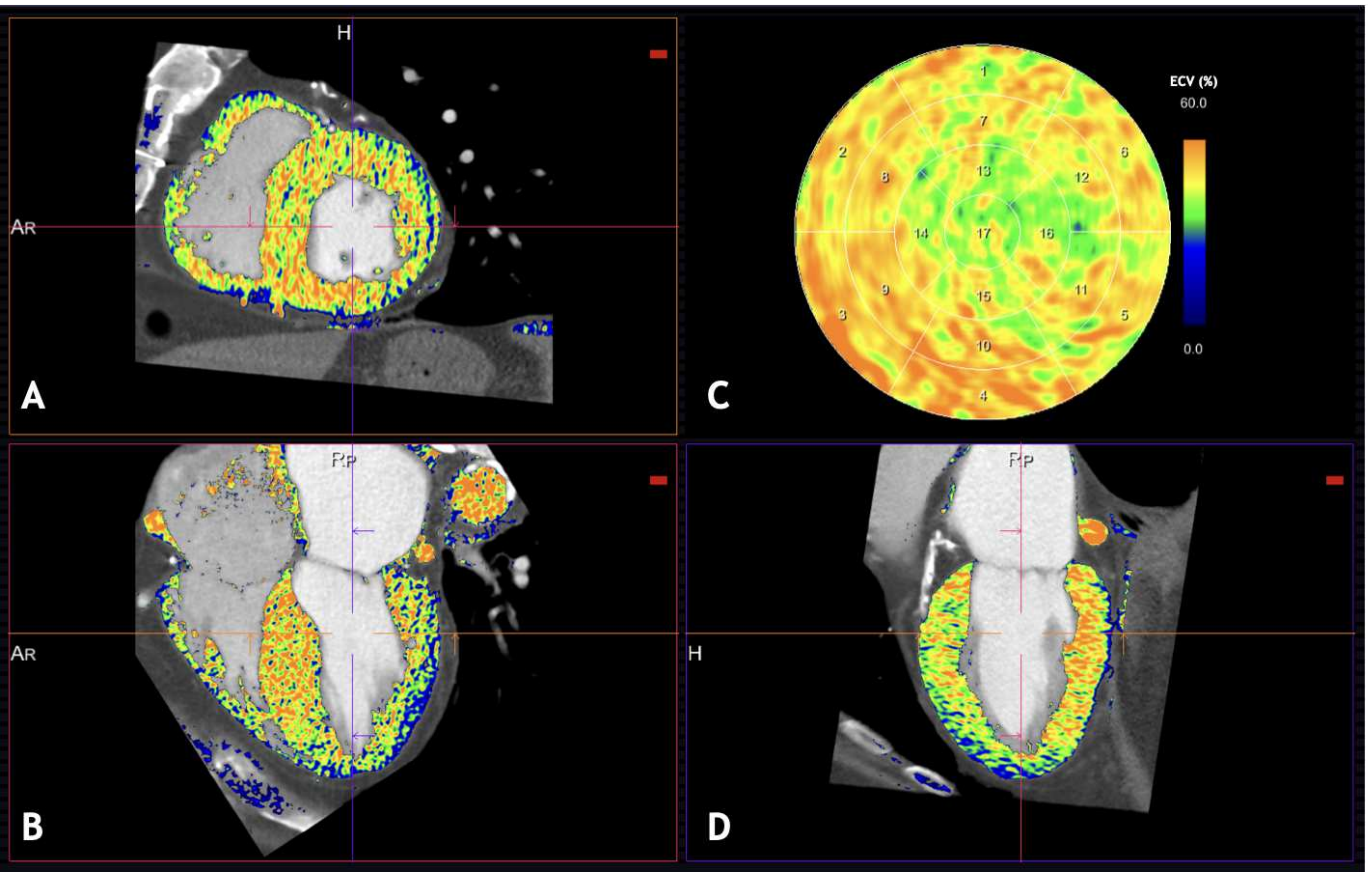
H
AR
A
ECV (%)
60.0
0.0
1
2
3
4
5
6
7
8
9
10
11
12
13
14
15
16
17
C
PP
AR
B
PP
H
D
E

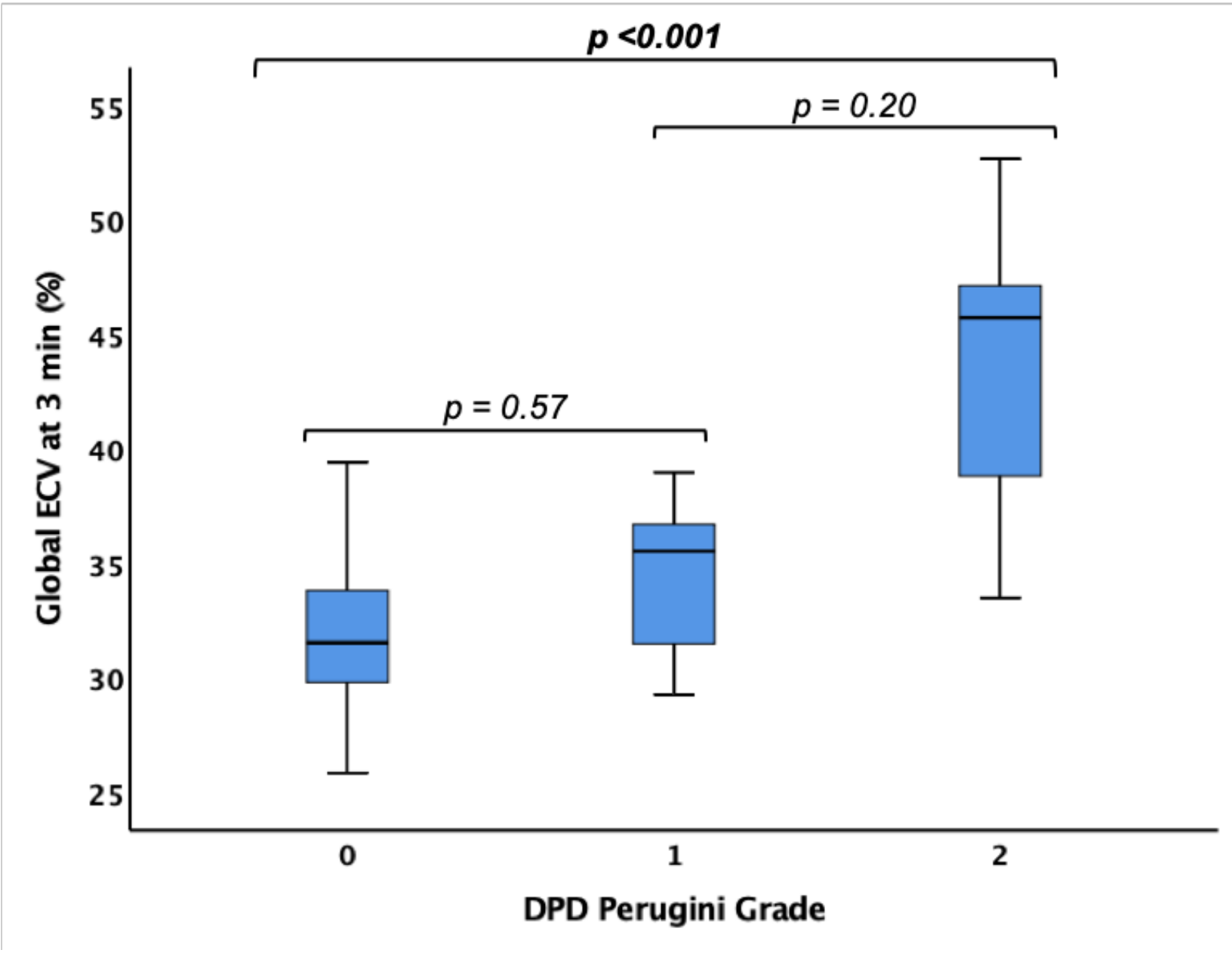
p <0.001
p = 0.20
p = 0.57
55
50
45
40
35
30
25
Global ECV at 3 min (%)
0
1
2
DPD Perugini Grade

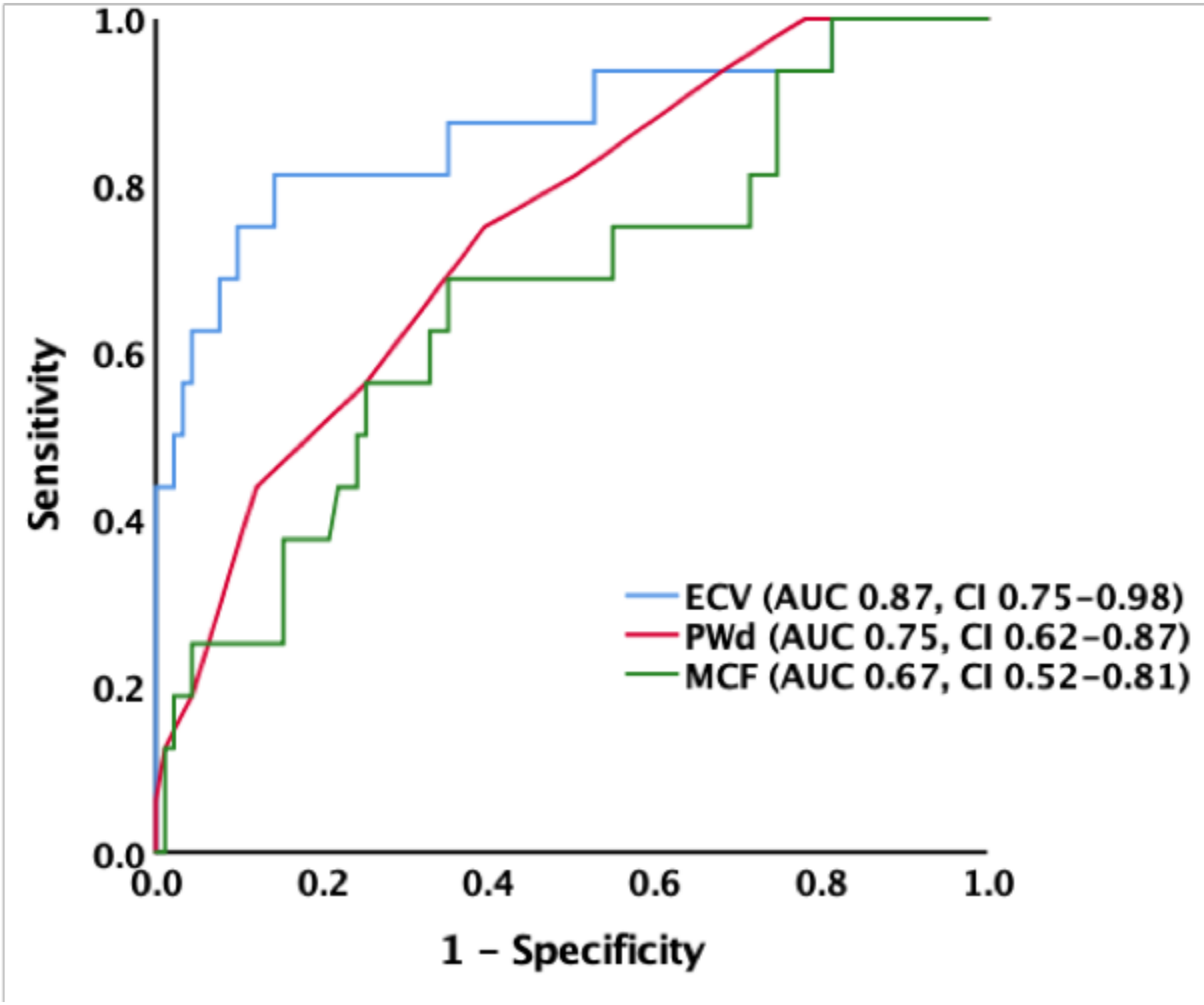
1.0
0.8
0.6
0.4
0.2
0.0
Sensitivity
0.0
0.2
0.4
0.6
0.8
1.0
1 – Specificity
ECV (AUC 0.87, CI 0.75–0.98)
PWd (AUC 0.75, CI 0.62–0.87)
MCF (AUC 0.67, CI 0.52–0.81)

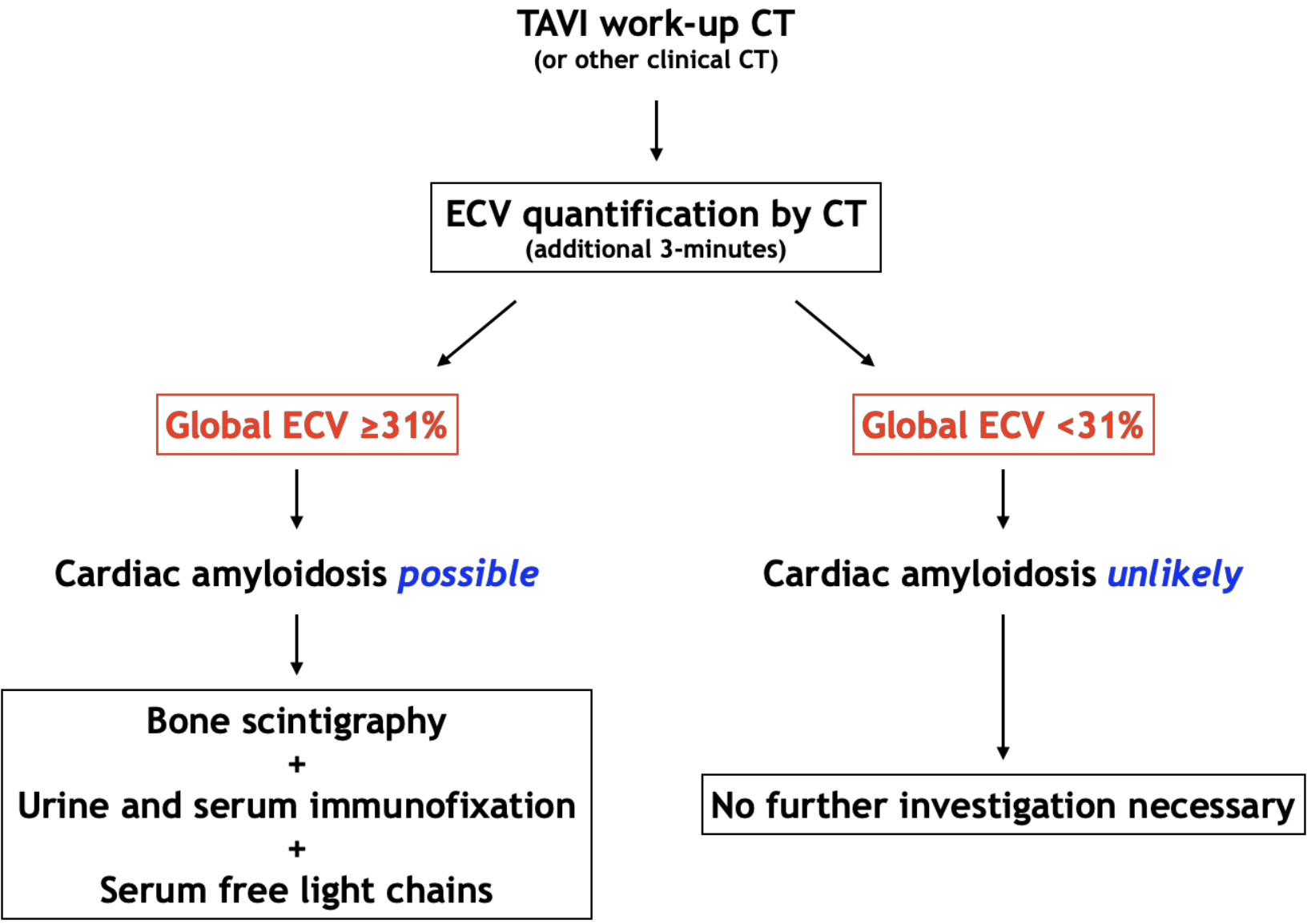
TAVI work-up CT
(or other clinical CT)
ECV quantification by CT
(additional 3-minutes)
Global ECV ≥31%
Global ECV <31%
Cardiac amyloidosis possible
Cardiac amyloidosis unlikely
Bone scintigraphy
+
Urine and serum immunofixation
+
Serum free light chains
No further investigation necessary

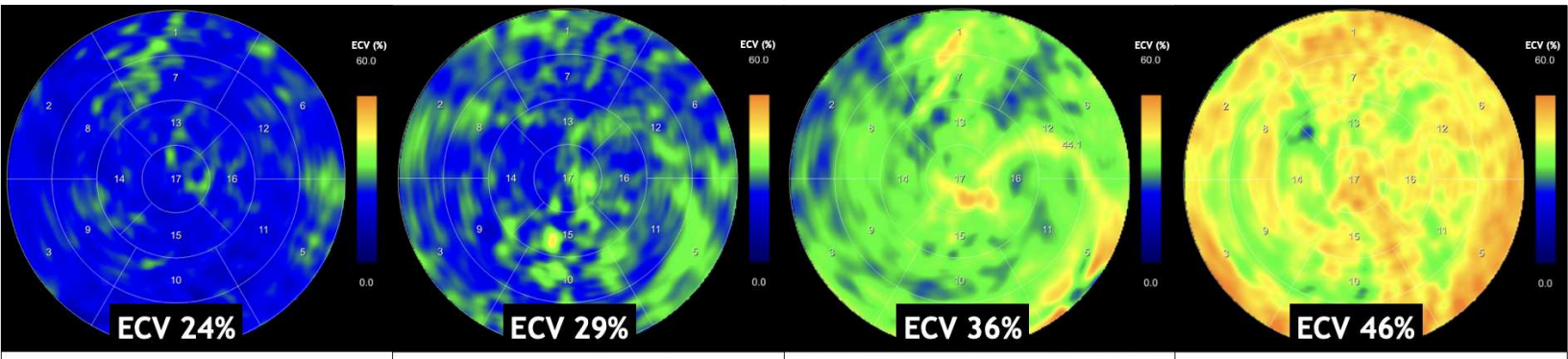

NOT DONE

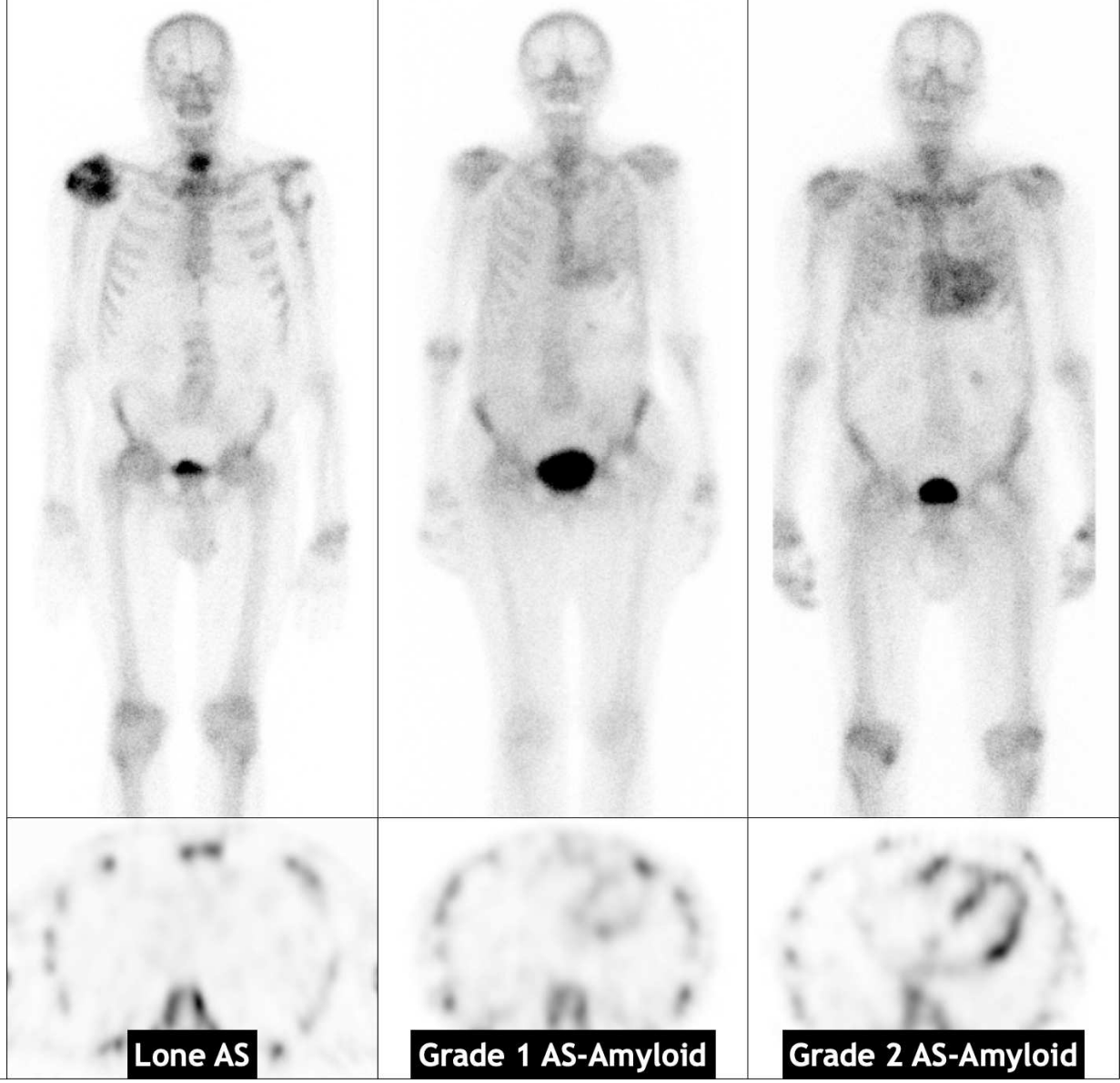

Control | Lone AS | Grade 1 AS-Amyloid | Grade 2 AS-Amyloid